Supplement for "An Overview of the Western United States Dynamically Downscaled Dataset (WUS-D3)"

[1]Stefan Rahimi, [1]Lei Huang, [1]Jesse Norris, [1]Alex Hall, [1]Naomi Goldenson, [1]Will Krantz, [1]Ben Bass, [1]Chad Thackeray, [1]Henry Lin, [1]Di Chen, [1]Eli Dennis, [2]Ethan Collins, [3]Zach Lebo, and [1]Emily Slinskey

[1]Center for Climate Science, University of California Los Angeles, Los Angeles, California, 90095, U.S.A.
[2]Department of Atmospheric Science, University of Wyoming, Laramie, Wyoming, 82071, U.S.A.
[3]School of Meteorology, University of Oklahoma, Norman, Oklahoma 73019, U.S.A.

Correspondence to: Stefan Rahimi (s.rahimi@ucla.edu)

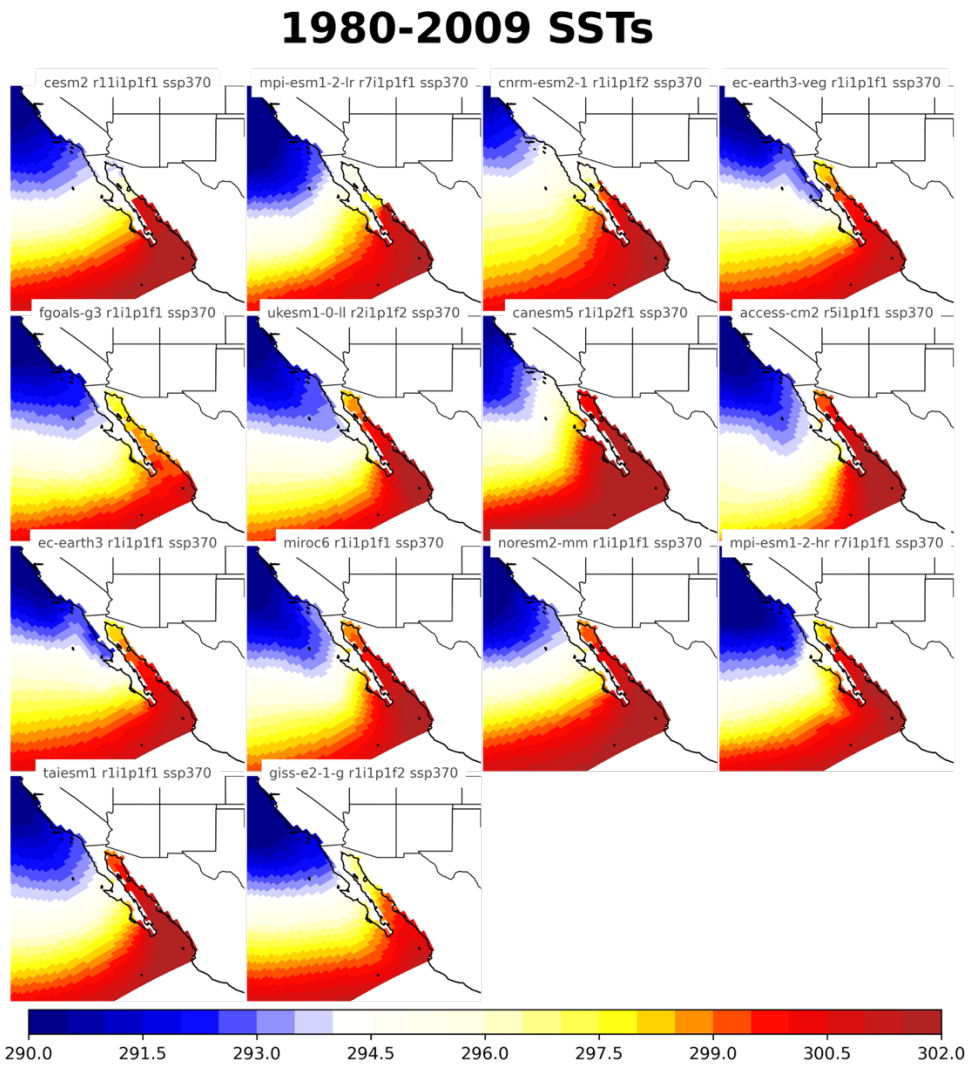

Figure S1. Annual-mean sea surface temperatures (SSTs; [K]) from 1980-2009 from 14 GCMs considered in this study

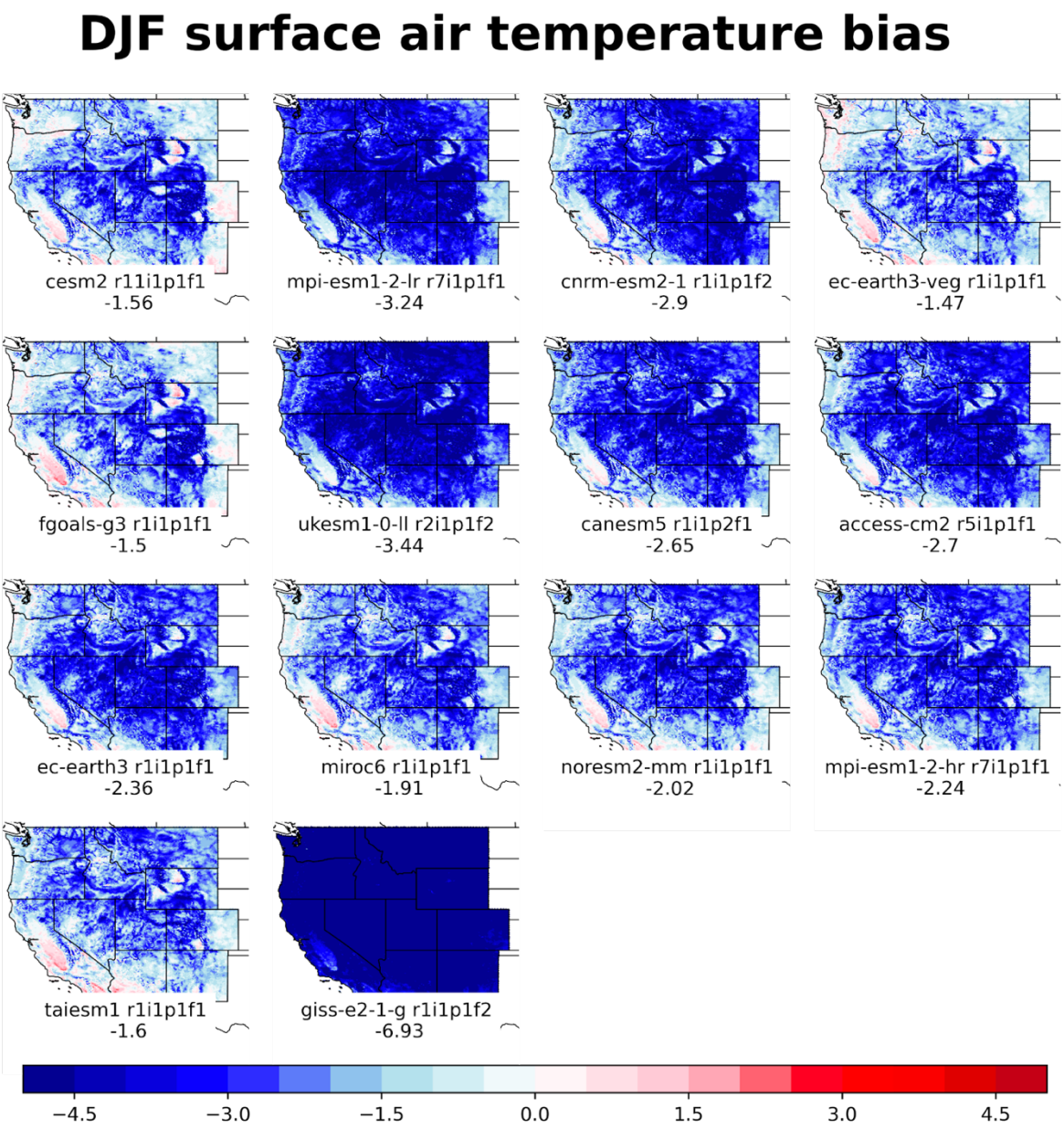

Figure S2. Wintertime (DJF) biases in dynamically downscaled surface air temperature from 1981-2010 relative to PRISM. 11-state-mean biases are presented beneath each GCM label [K].

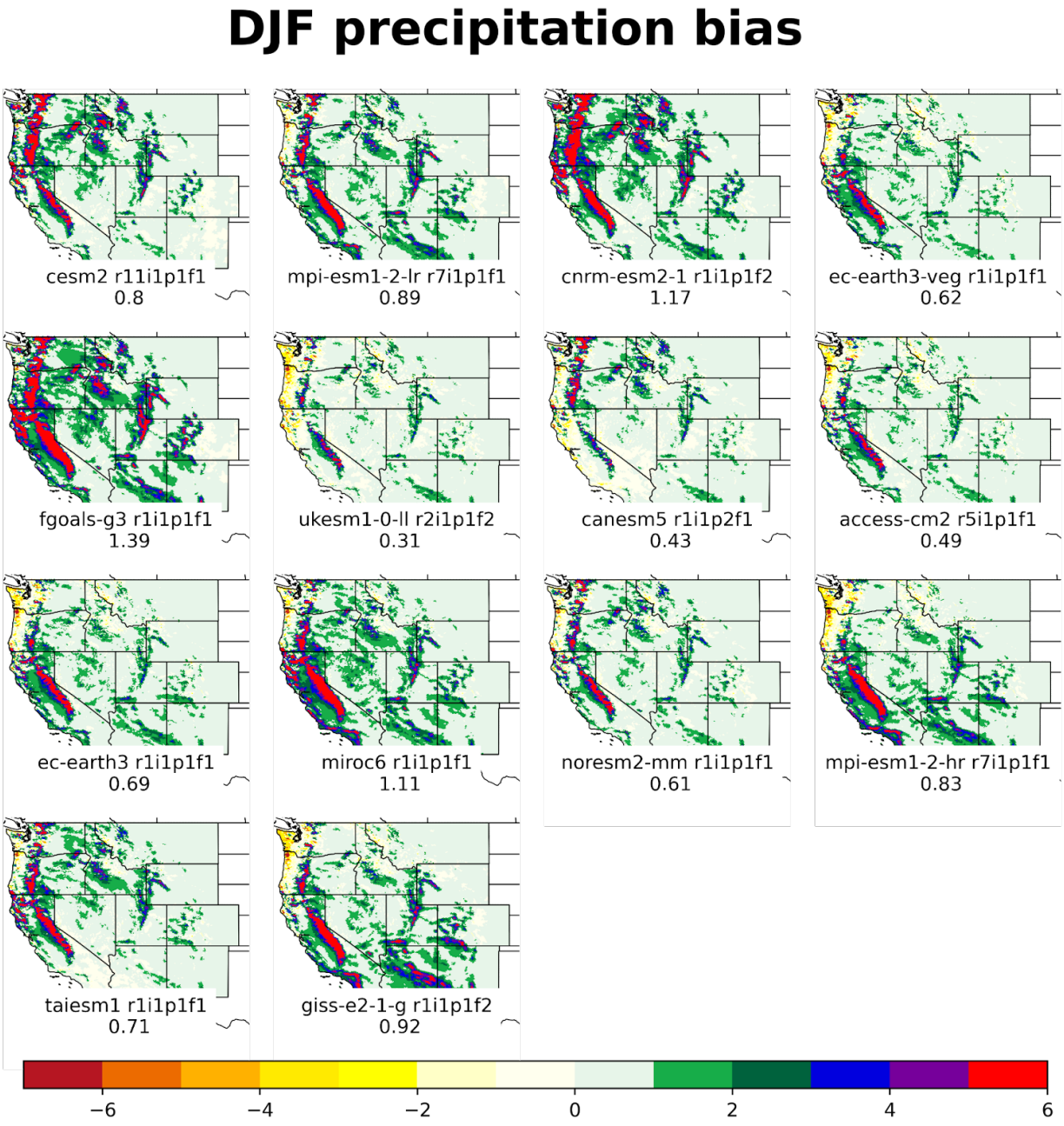

Figure S3. **Same as in Fig. S2, but for precipitation rate [mm d^{-1}].**

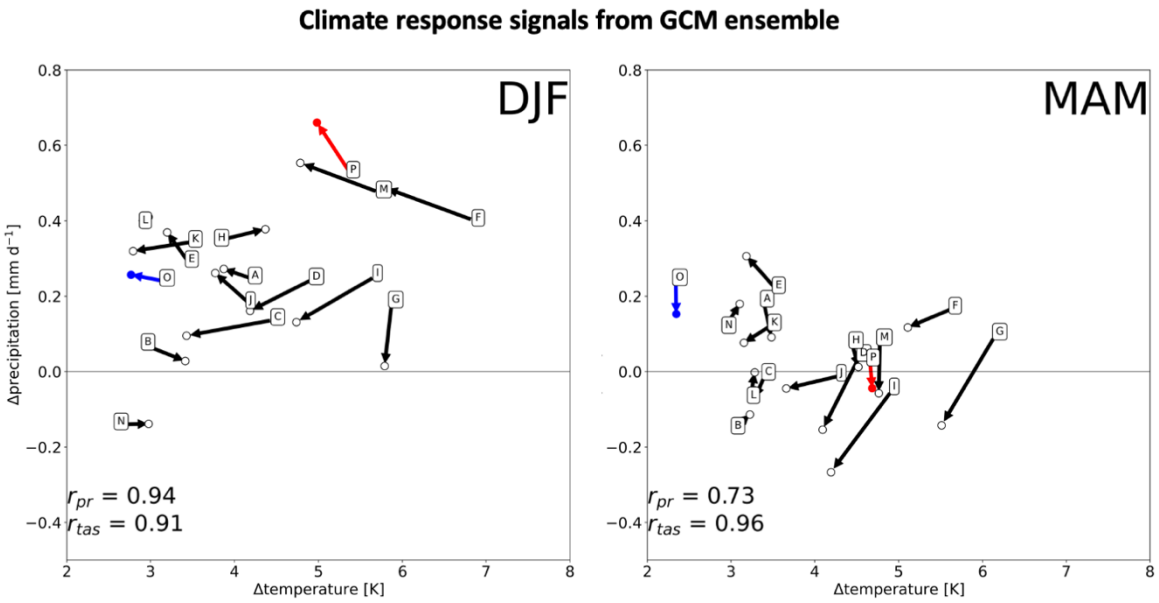

Figure S4. Future winter (DJF) and springtime (MAM) climate response for parent GCMs (indicated by lettering) and their downscaled counterparts (indicated by circles) on the 9-km WRF grid averaged across 11 western U.S. states (End-Century). Non-colored circles are for SSP3-7.0 projections only, while blue (red) circles represent the SSP2-4.5 (SSP5-8.5) projections. Arrows point away from parent GCMs towards downscaled counterparts.

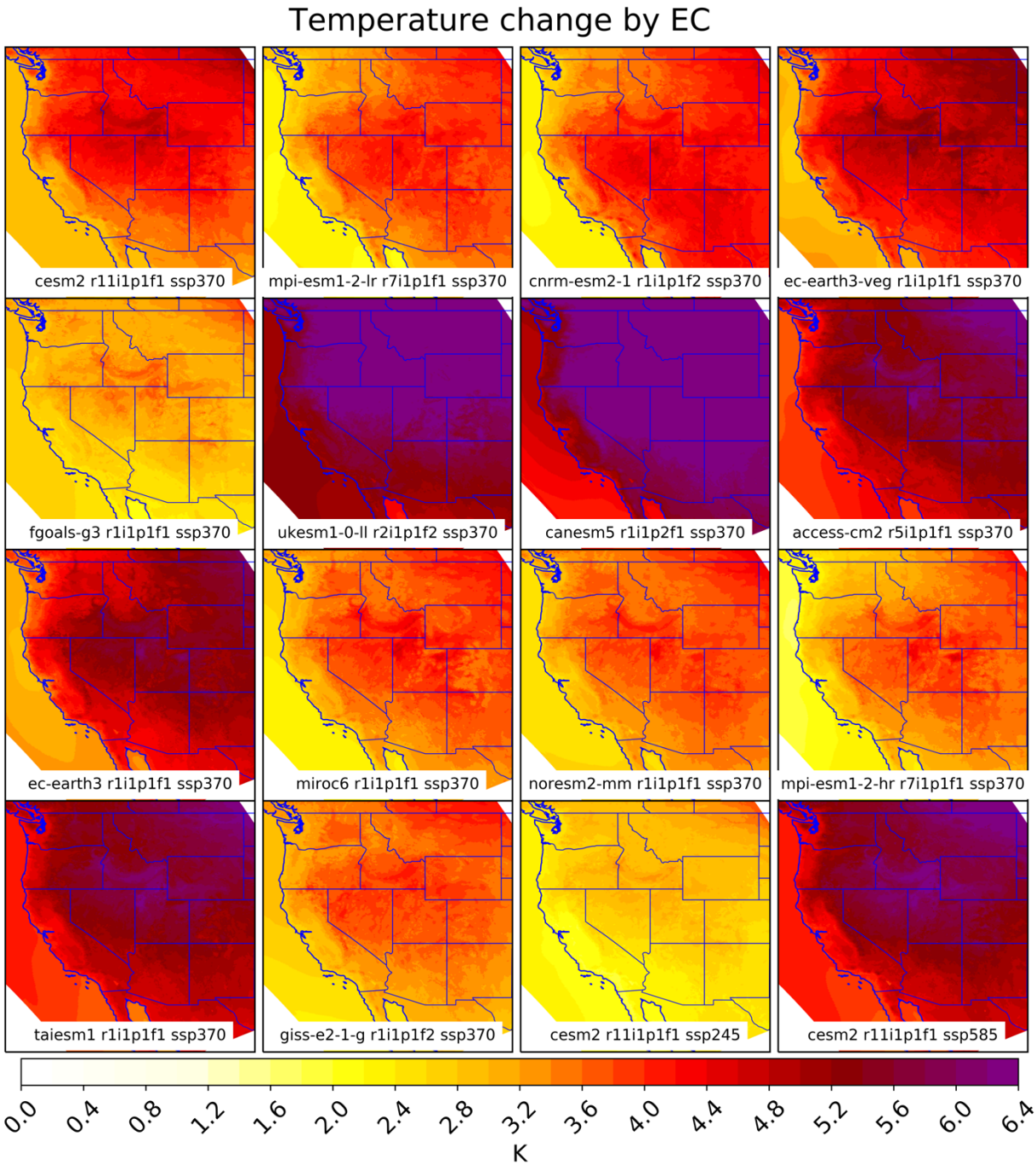

Figure S5. Changes in annual-mean surface air temperature by the end-of-century (2070-2100) period.

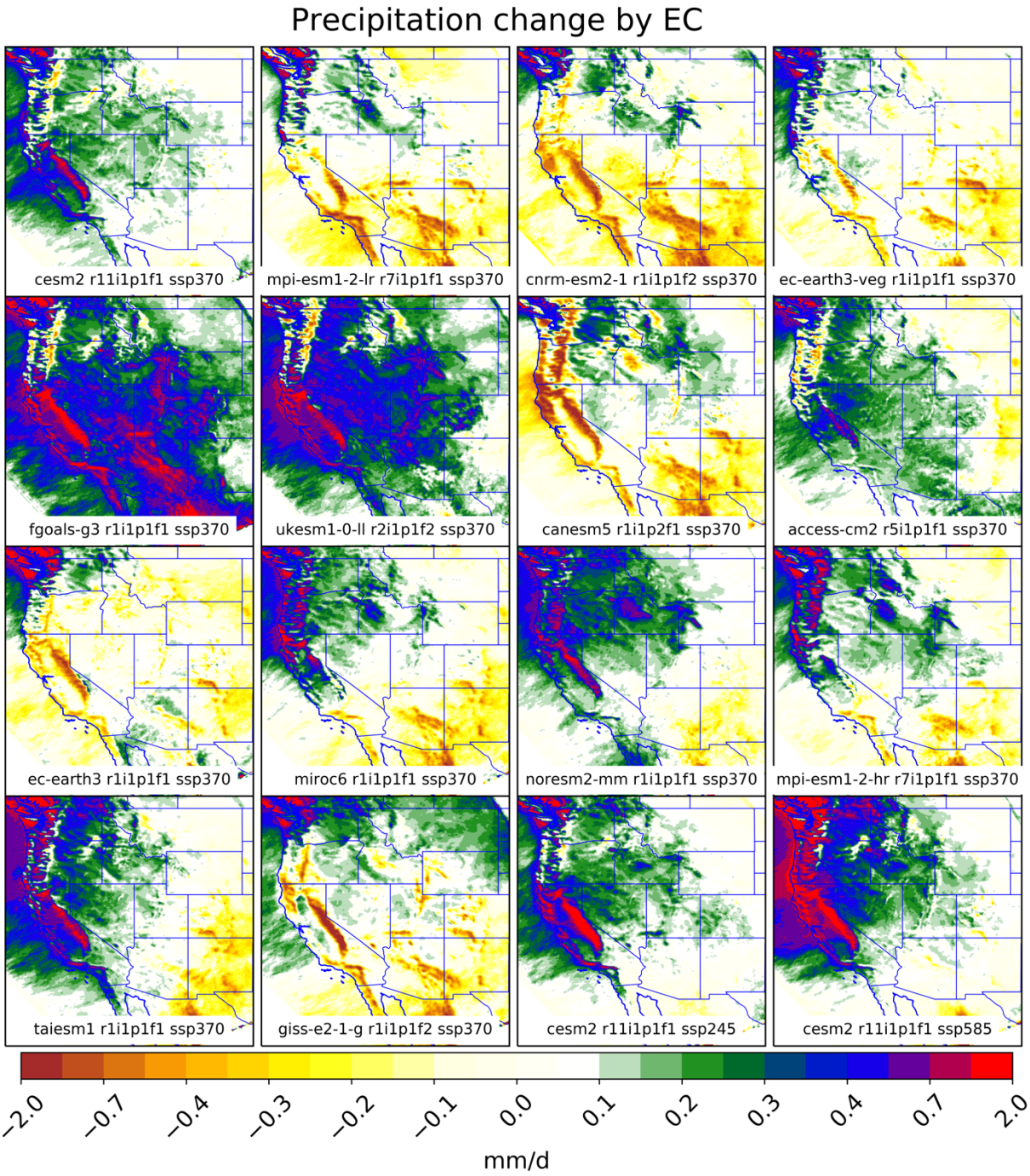

Figure S6. Same as in Fig. S5, but for precipitation [mm d^{-1}].

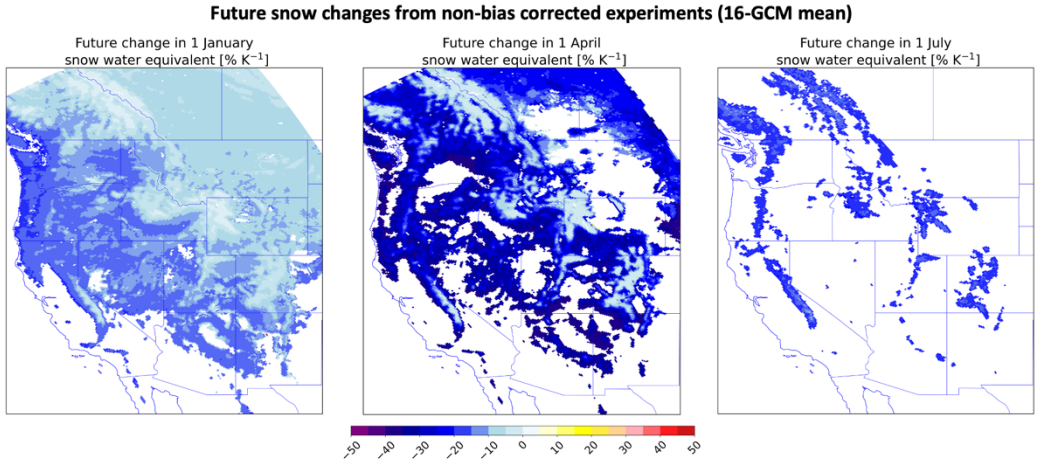

Figure S7. Future changes in 1 April snow water equivalent normalized by the amount of global warming [% K^{-1}] in th 16-GCM mean.

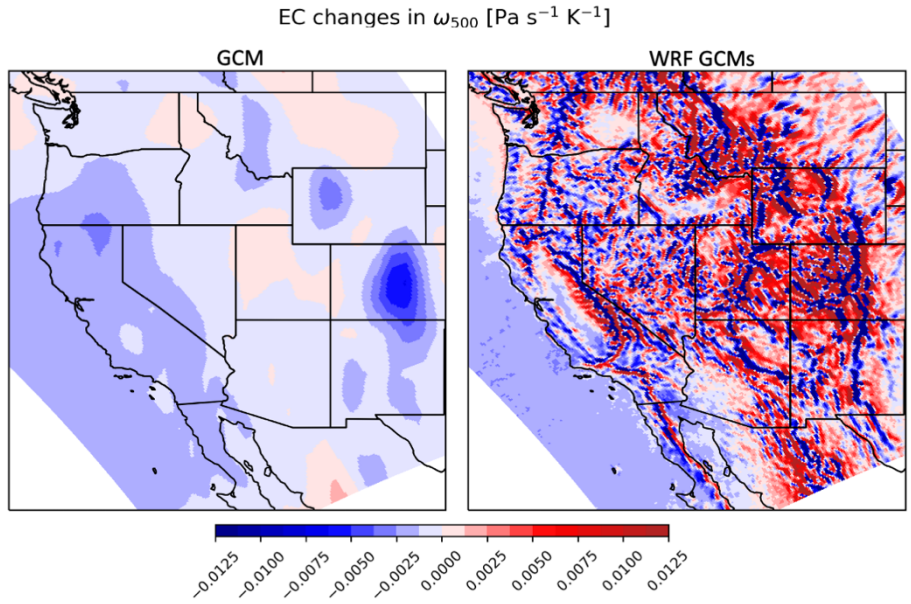

Figure S8. Ensemble-mean future changes in 500 hPa pressure velocity normalized by end-of-century (2070-2100) mean global warming [Pa s^{-1} K^{-1}].

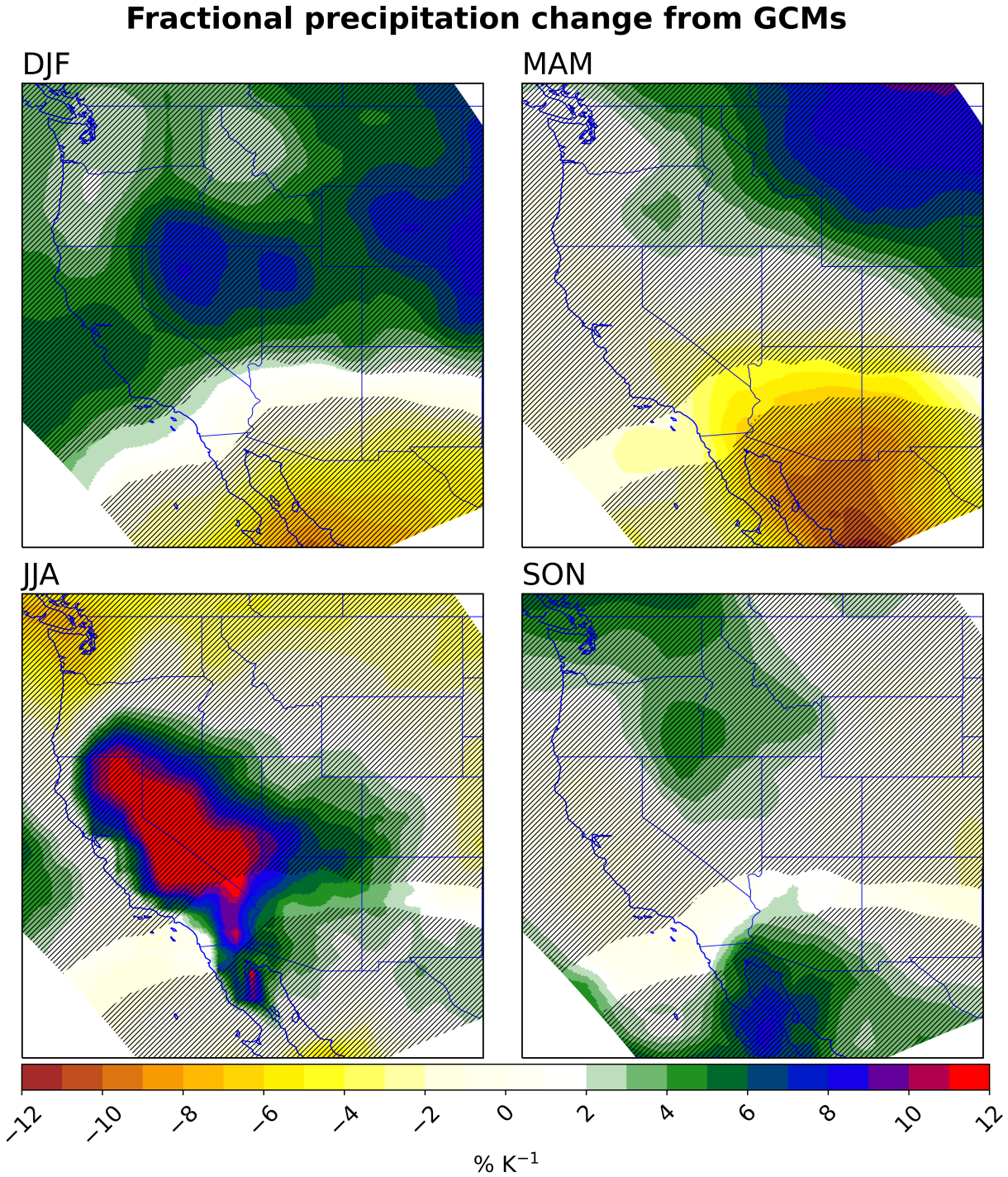

Figure S9. 16-GCM-mean future changes in native-GCM fractional precipitation normalized by the amount of global warming [% K^{-1}]. Hatching indicates statistical significance to the 95% confidence interval when grid point distributions are subjected to a two-sided Student's t-test. Stippling is not included for temperature because every grid point returns a p value smaller than 0.05.

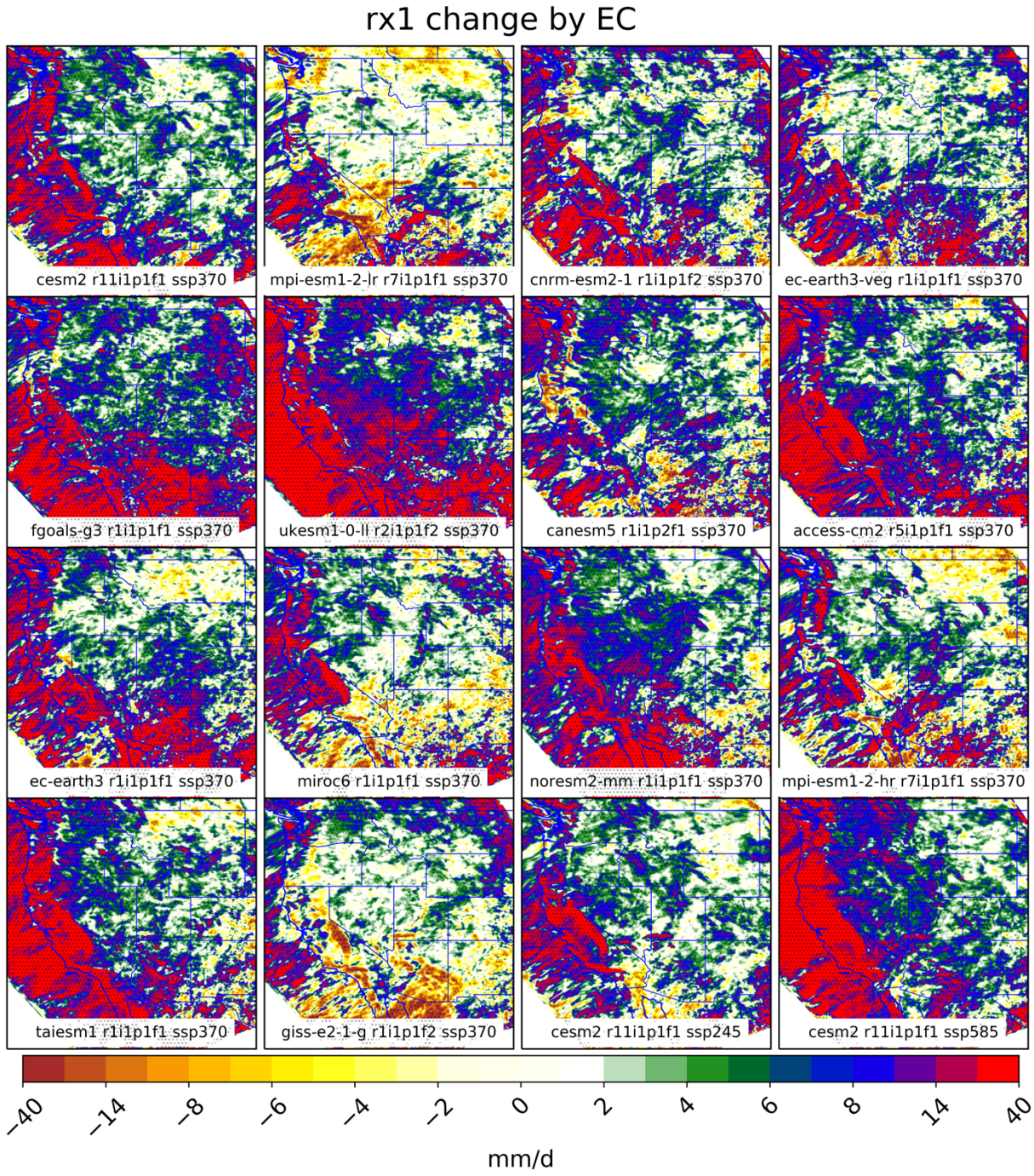

Figure 10. End-of-century (2070-2100) changes in rx1day precipitation for each GCM [mm d^{-1}]. Circles denote statistical significance to the 95% for a two-sided Student's t-test.

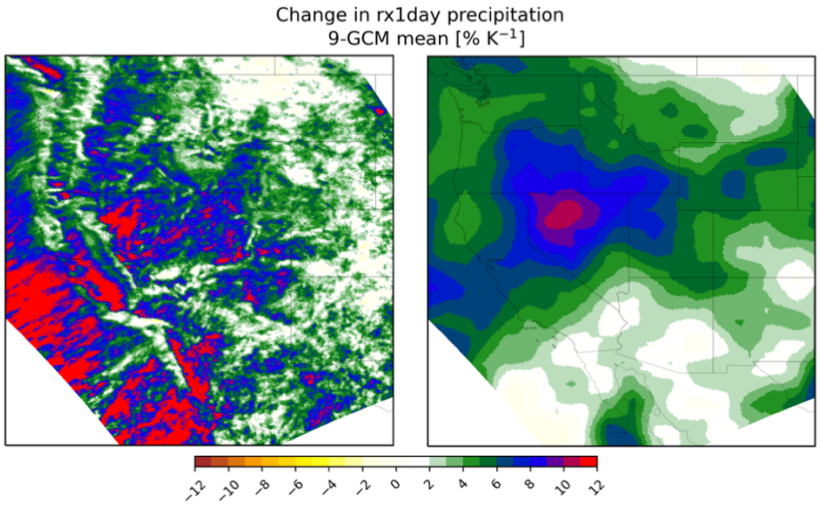

Figure S11. Future change in (left) WRF and (right) GCM rx1day precipitation considering a 9-GCM mean [% K^{-1}].

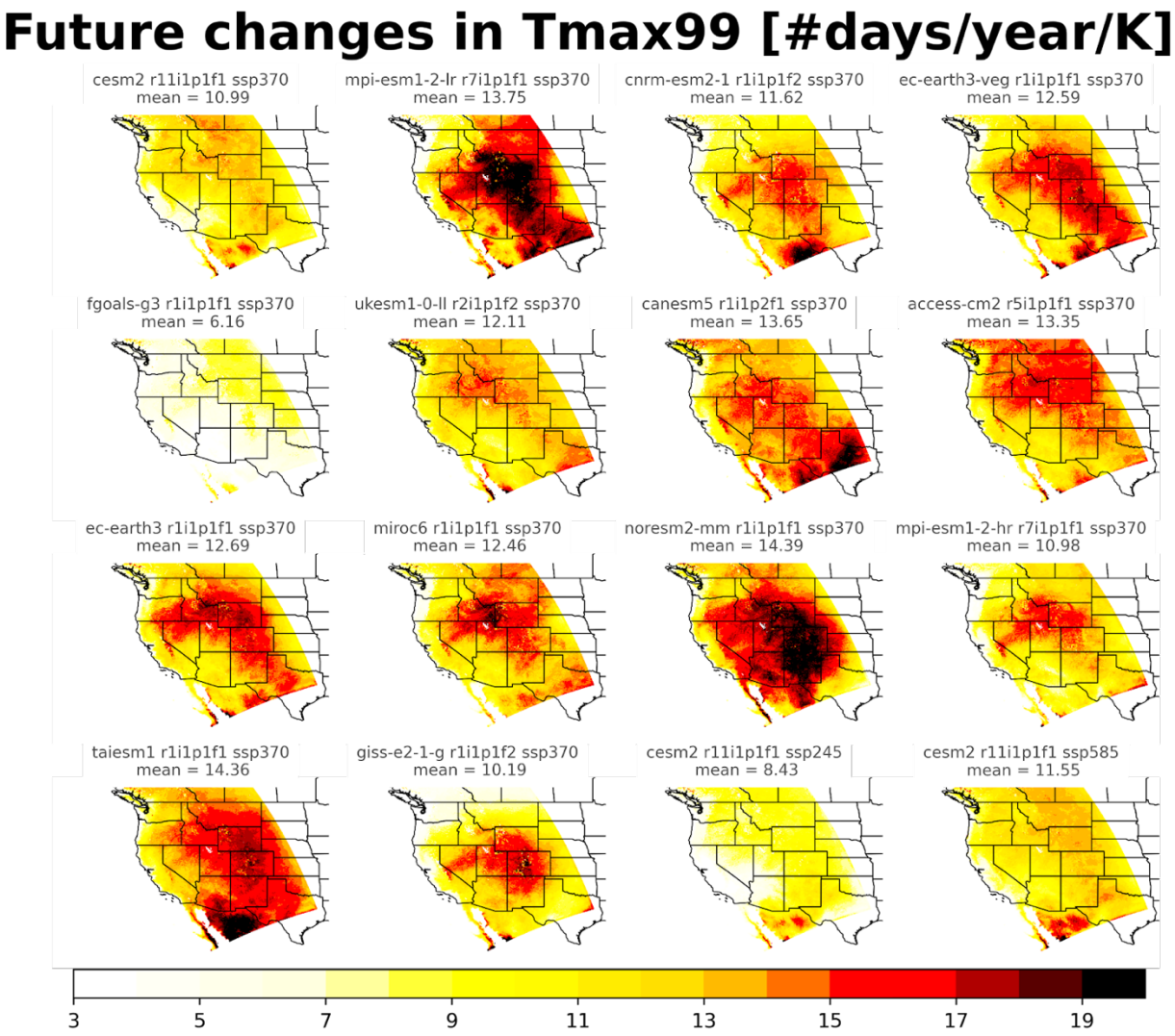

Figure S12. Future changes in maximum daily 99th percentile surface air temperature (Tmax99) per degree of global warming [days year^{-1} K^{-1}] for each downscaled GCM.

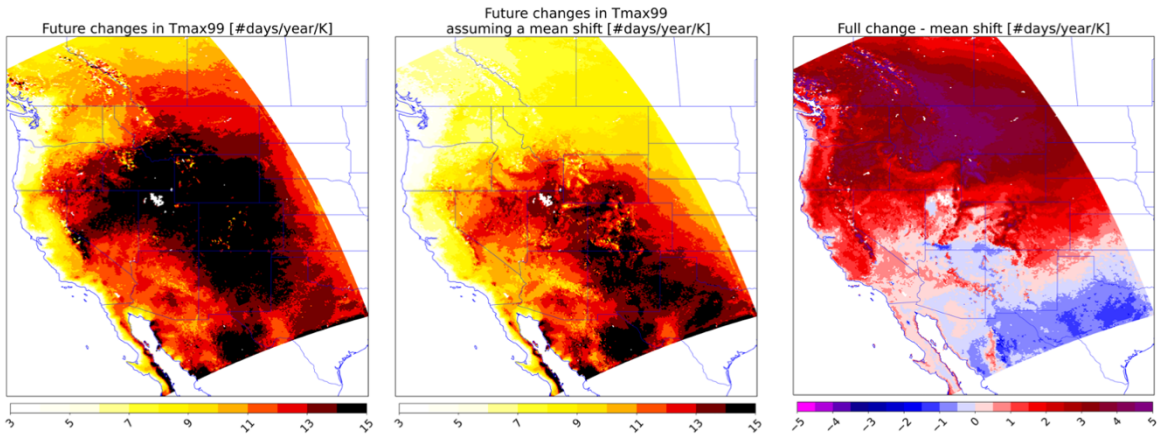

Figure S13. 11-GCM future changes in maximum daily 99th percentile surface air temperature (Tmax99) per degree of global warming [days year^{-1} K^{-1}] considering the full change (left) and assuming a mean shift in the temperature distribution (middle). The right panel presents the difference between the left and center panels.